FLAX FIBERS FOR STRENGTHENING OF TIMBER STRUCTURES FINITE ELEMENT MODELLING

Alann André[1] and Helena Johnsson[2]

[1] SWEREA SICOMP AB, Box 104, 431 22 Mölndal, Sweden, alann.andre@swerea.se
[2] Luleå University of Technology. Dept. of Civil and Environmental Engineering, LULEÅ, Sweden

ABSTRACT

A Finite Element Analysis (FEA) was carried out to model small prismatic glulam specimens reinforced with flax fibers composites in the direction perpendicular to the grain. Two-dimensional models were used to study the elastic and the softening response of the specimens. Damage and crack opening was modelled based on the "fictitious crack model". Cohesive elements together with a traction separation law were used. The model of glulam specimen where high tensile stresses perpendicular to grain are expected should consider the cylindrical orthotropy (annual rings) assumption. The tensile stresses perpendicular to grain obtained with FEA can be compared to those from experiments. Cohesive interface elements have been used successfully to model the crack formation and propagation in glulam under tension perpendicular to the grain.

1. INTRODUCTION

Wood has its weakest mechanical property in tension perpendicular to the grain [1]. For glulam, the characteristic value of the tension perpendicular to the grain $f_{t,90,k}$ can be 60 times lower than for tension parallel to the grain $f_{t,0,k}$. Therefore, a great interest to control this drawback has been the focus of many projects. Double tapered beams, for instance, present a curvilinear bending stress distribution in almost all sections, resulting in tension perpendicular to the grain at the apex area ([2],[3]).

There is today a necessity to increase, maintain and upgrade old wooden structures and to allow new structures using wood and glulam. Larsen et al. [4] studied the effect of reinforcing curved and pitched cambered glulam beams perpendicular to the grain with glass fibre mats. The fibres were randomly oriented in the laminate and the laminate was bonded to the side of the beam in the apex area. It was shown that FRP could increase the tensile strength perpendicular to the grain and that the failure mode switched from brittle in tension perpendicular to the grain to semi-ductile in bending or shear.

Reinforcement can have major advantages; increase of the mechanical properties, decrease of the wooden member dimensions, use of lower wood grades and a more ductile behavior of the reinforced system.

During the last years, reinforcement of glulam has been one of the more intense research areas in timber engineering. High strength fibres (aramide fibres, carbon fibres and glass fibres) have been used. These fibres are stiff and strong, have low density and are corrosion resistant. Flexural, shear, compressive or tensile strengthening of timber beams have been achieved ([4]-[6]).

However, the use of petroleum or mineral based fibres in FRP components makes them difficult to recycle. Today, the pressure from society to use sustainable, renewable natural materials has considerably increased. Natural fibres such as flax, hemp, henequen, jute, kenaf, sisal, etc. fit well in this approach: they are light, renewable,

CO_2-neutral and possess interesting specific mechanical properties. These characteristics make them possible to use for strengthening of wooden structural elements.
The objective of this study was to investigate the use of flax fibres composites as reinforcement for glulam in tension perpendicular to the grain and to study the damage initiation and propagation in glulam using finite element analysis and cohesive elements. The study objects are prismatic glulam specimens loaded in tension.

2. EXPERIMENTS

Six prismatic glulam specimens, $405\times223\times115\,mm$, with a reference volume of V_0=0.01m^3, [7], reinforced with flax fibre reinforced polymer (FFRP) composites (0.7 mm thick, one layer), and six unreinforced specimens were tested to failure in tension perpendicular to the grain. All specimens were previously conditioned at (20±1)ºC and (30±10)% relative humidity in a climate room. The testing equipment used was a Dartec Ltd RE 8991 machine with a 600 kN load cell (Figure 1). The tests were conducted in displacement control mode, and the rate was 0.15mm/min for all specimens. Two Linear Variable Displacement Transducers (LVDT) with a 240 mm gauge length were used to measure the displacement in the load direction.

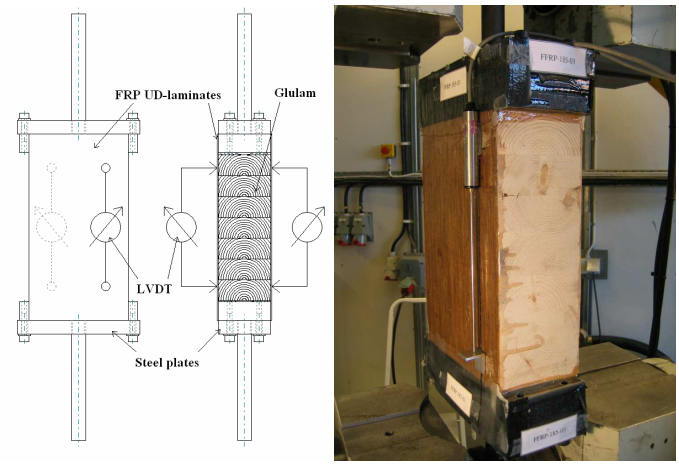

Figure 1: Test set-up for prismatic glulam specimen

3. FINITE ELEMENT MODEL

Timber is usually modelled using a linear stress analysis [8]. The material is considered as brittle with deterministic properties and a stress based failure criteria is used. Wood is a material that presents a softening behaviour [9]. The fictitious crack model [10], which is a non linear fracture mechanics representation (NLFM), is considered herein based on the fracture energy of timber ($G_f \neq 0$). The crack forms and propagates in the RL-orientation (Radial-Longitudinal). Gradual damage and fracture performance of timber have been studied ([9],[11],[12]). The critical energy released in fracture mode I has been found to be strongly dependent on the wood density ρ [12].

$$G_{Ic} = -146 + 1.04\rho \qquad (1)$$

For softwood, a density between 400 and 600 kg/m^3 is reported [13], which corresponds to the fracture energy G_{Ic} varying between 270 and 478 Nm/m^2.
The fictitious crack model has been used mostly for concrete fracture processes but has also been extended to wood. Contrary to linear fracture mechanics, it is assumed that the crack occurs in a plane (interface) where the variation of cohesive stresses,

governed by a specific traction separation law, generates the damage of the material and the decrease of stress transfer.
Cohesive elements are usually used to model the behaviour of interfaces (between layers in composites, adhesive joints, etc.). A model with cohesive elements does not need an initial crack; the place where damage initiates first is a part of the analysis. In the case of wood and fracture perpendicular to the grain, a crack propagates in the same section as it starts and parallel to the fibres. The cracked section is not strictly perpendicular to the load axis (Figure 2). Indeed, the crack propagates at an angle to the orientation of the annual rings and perpendicular to latewood, which creates a wavy pattern between annual rings [1]. For simplicity, crack propagation in a plane perpendicular to the load direction is assumed.

Figure 2: Crack path in unreinforced specimen

The crack propagation is caused by high stresses perpendicular to the grain in that plane. Cohesive elements were used together with a traction separation law (TSL), which defines the traction function of the separation distance between interface elements. The material has an initial linear elastic behaviour. The elastic response is followed by damage initiation and evolution until total degradation of the elements.
The quadratic nominal stress criterion was used as the damage initiation criterion, Equation (4). The maximum values of the nominal stress allowed before degradation (strength) are chosen as material properties and are denoted t_i^0.

$$\left\{\frac{\langle t_n \rangle}{t_n^0}\right\}^2 + \left\{\frac{t_s}{t_s^0}\right\}^2 + \left\{\frac{t_t}{t_t^0}\right\}^2 = 1 \qquad (4)$$

The damage evolution of a material can be based on energy dissipation or on effective displacement. In both cases, the idea is to determine the rate of material stiffness degradation. A damage variable D together with predicted values of the stress components at the same strains without damage $\bar{t}_i$ are used to determine the stress components after the damage criterion is fulfilled (t_i), Equation (5).

$$t_i = (1-D)\bar{t}_i \qquad (5)$$

The fracture energy G_f represents the energy released under damage evolution, and is graphically the area under the traction separation curve (Figure 3). The element is totally degraded when the damage parameter D is equal to one. The stress component t_i^0 is then zero.

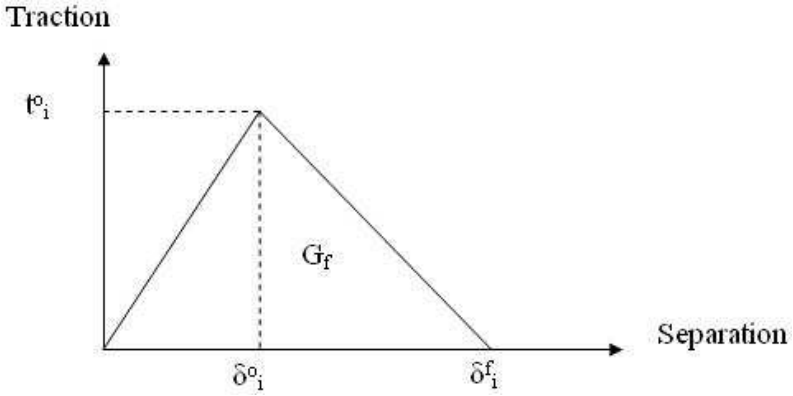

Figure 3: Traction separation response

When fracture energy governs damage evolution in a linear traction separation response, the damage parameter is described as:

$$D = \frac{\delta_i^f .\left(\delta_i^{\max} - \delta_i^0\right)}{\delta_i^{\max} .\left(\delta_i^f - \delta_i^0\right)} \quad \text{where } \delta_i^f = \frac{2G_f}{t_i^0} \qquad \text{(6) and (7)}$$

4. EXPERIMENTAL RESULTS

The results are presented in Table 1 in terms of maximum load, maximum displacement and failure mode. Failure modes A and B correspond respectively to failure of the glulam perpendicular to the grain and failure of the glulam perpendicular to the grain followed by fibre failure of the composite.

Table 1: Experimental results

Name	Failure load (kN)		Max. Displacement at failure (mm)						Failure mode
			LVDT 1		LVDT2		Stroke		
	G^1	S^2	G^1	S^2	G^1	S^2	G^1	S^2	
UNR-01	13.15		-		1.00		0.94		A
UNR-02	11.54		0.41		0.36		0.67		A
UNR-03	20.03		0.67		0.71		1.14		A
UNR-04	28.28		0.88		0.89		1.50		A
UNR-05	22.99		0.67		0.56		1.00		A
UNR-06	26.14		0.70		0.88		1.28		A
FFRP-01	27.25	28.54	0.88	1.07	0.96	1.01	1.48	1.62	B
FFRP-02	28.28	32.68	0.60	1.19	0.49	1.09	1.02	1.71	B
FFRP-03	27.17	29.82	0.50	1.01	0.68	1.27	1.08	1.67	B
FFRP-04	17.41	33.91	0.59	1.31	0.51	1.20	0.86	1.88	B
FFRP-05	31.07	35.47	0.66	1.31	0.64	1.43	1.35	2.13	B
FFRP-06	24.12	33.43	0.47	1.34	0.41	1.15	0.88	1.88	B

The average value along the cross section of the tensile strength perpendicular to the grain before failure in the glulam has been calculated using the failure loads and the stressed area of the specimens (Table 2).

Table 2: Maximum stress at glulam failure

	Unreinforced	FFRP
Mean (MPa)	0.79	0.99
Standard deviation (MPa)	0.27	0.18
Average displ. (mm)	0.67	0.62

The maximum tensile stress perpendicular to the grain increased by +25% when FFRP was applied. It is interesting to note that the maximum displacement at failure is comparable.
From the experimental results, the tensile modulus perpendicular to grain E_{90} has been determined for each specimen based on the recorded displacement. The stiffness of the specimens increased for all strengthened specimens. The use of FFRP enhanced the stiffness by +32 %. The load displacement curves for some of the unreinforced and FFRP reinforced specimens are shown in figures 4.

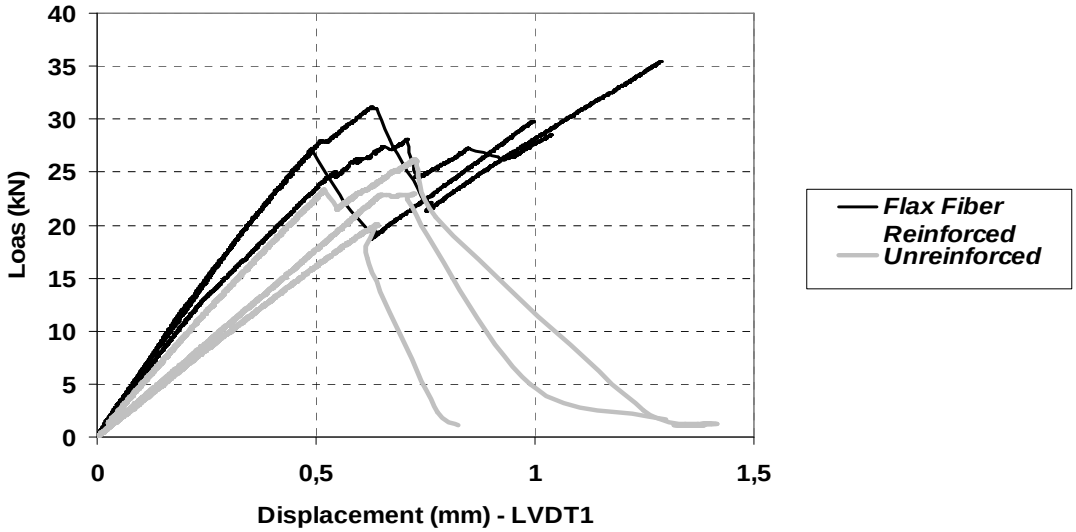

Figure 4: Load-displacement curves for experimental results

5. FINITE ELEMENT MODELLING

Linear elastic models

The prismatic glulam specimen was modelled using the commercial finite element software ABAQUS [14]. Three different materials were identified and characterized: the timber, the cohesive interface and the reinforcement. The cohesive interface was assigned values based on experimental results and the literature, Table 3. The glulam was considered defect free, i.e. local inhomogeneities such as knots, slope of grain, compressive wood, etc. were neglected. The engineering constants for the FFRP were determined from experiments.

Table 3: Material properties

Glulam L-40 [8					
$\mathbf{E_L}$	14 000 MPa	$\mathbf{G_{LR}}$	800 MPa	$\mathbf{\upsilon_{LR}}$	0.02
$\mathbf{E_R}$	800 MPa	$\mathbf{G_{LT}}$	500 MPa	$\mathbf{\upsilon_{LT}}$	0.02
$\mathbf{E_T}$	500 MPa	$\mathbf{G_{RT}}$	60 MPa	$\mathbf{\upsilon_{RT}}$	0.45
FFRP (from experiments)					
$\mathbf{E_L}$	13 012 MPa	$\mathbf{G_{LT}}$	1119 MPa	$\mathbf{\upsilon_{LT}}$	0.34
$\mathbf{E_T}$	4 017 MPa			$\mathbf{\upsilon_{TL}}$	0.10
Cohesive interface					
Elastic properties	**E (MPa)**	**G_1 (MPa)**	**G_2 (MPa)**		
	800	800	500	*[8]*	
Damage criterion	**$f_{t,90}$ (MPa)**	**f_v (MPa)**		*from experiments and [1]*	
	0.7 – 0.4	3			
Damage evolution	**G_f (N/m)**			*[12]*	
	370 – 200				

The cylindrical orthotropy assumption is used in the 2D model. The origin of the cylindrical coordinate system was assume to be situated at a distance d = 30 mm from the lower side of each lamination.
The distribution of the stress perpendicular to the grain at mid-height was investigated at an applied load of 19 kN. The maximum stress perpendicular to the grain is situated at mid-width and is equal to 1.64 MPa. The tensile stress distribution perpendicular to the grain is uneven, and lower values are observed near the outer edges. Experimental results gave a mean value of 0.79 MPa and Blass et al. [15] reported a mean value of 0.82 MPa.
The FFRP was added to the 2D-model and considered perfectly bonded to the glulam. An exploded view of the assembly is shown in Figure 6.

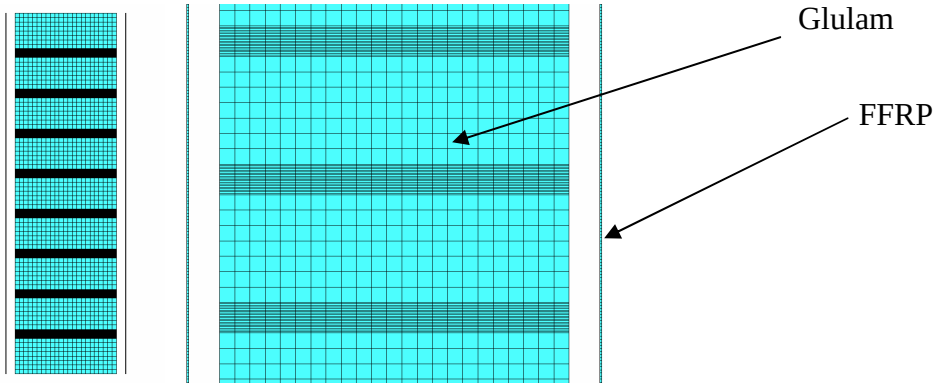

Figure 6: Assembly glulam-FFRP and mesh.

The load displacement curve is plotted and compared to unreinforced specimens in Figure 7. The stiffness of FFRP reinforced glulam specimens is higher than unreinforced specimens, which was also noticed during experiments.
From the experimental result, the failure load of FFRP reinforced glulam has an average value of 26 kN. It was shown from the FEA that at this load, the tensile stress perpendicular to the grain in the FFRP reinforced glulam reached a peak value (1.51 MPa) comparable to the maximum value reported for unreinforced specimen at 19 kN. The application of FFRP decreased the maximum tensile stress perpendicular to the grain by 26 %, and the failure load increased by 37%.

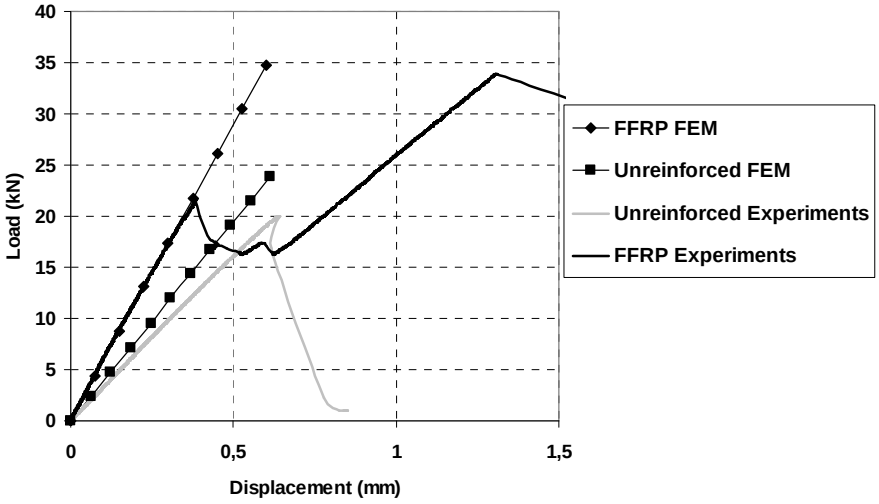

Figure 7: Load displacement curves for FFRP reinforced and unreinforced specimens

Longitudinal stresses in the FFRP are not constant along the height of the specimen. Higher stresses are situated at mid-height. At the level of one lamination, and in a similar pattern for all laminations of the specimen, higher stresses are observed at the interfaces between laminations.
Higher stiffness is predicted for unreinforced specimens with the FE model. Regarding the specimens reinforced with FFRP, the stiffness from the FE model is in good agreement with the experiments.

Damage modelling
In the damage modelling, the crack is assumed to occur in the middle lamella (since the wood is free from defects, there is no weakest section). The cohesive interface was positioned in a section close to the bottom lamination interface. In reality, it was shown that most of the cracks propagated from the interface between two lamellas on a rather long distance if compared to the width (Figure 2).
During the experiment, most of the specimens had from the beginning a weak section characterized by defects present inside the wood. Most of the cracks propagated from these defects. In the model, the glulam was considered free from defects and the crack needed to open after the critical energy was reached and then propagation occurred.
Contour plots of the crack propagation under loading for unreinforced and FFRP reinforced specimens are shown in Figure 9 and 10 respectively (deformation scale factor=50).

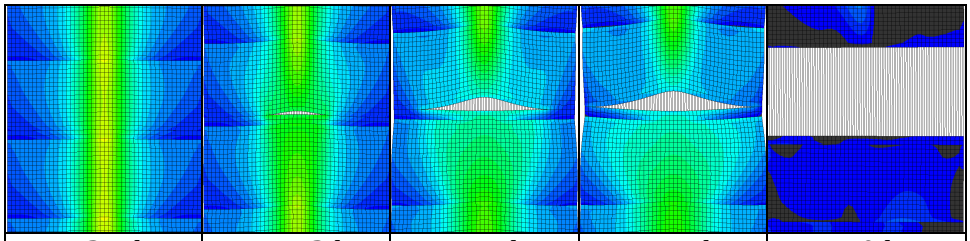

Figure 9: Crack propagation for unreinforced specimen.

For unreinforced specimens, the crack forms around 11 kN in the middle of the width and propagates in both directions towards the outer edges. The load still increases while the crack propagates. The load starts to decrease around 17 kN, until total degradation of all cohesive elements.
The FFRP reinforced model shows a decrease of the load until the FFRP takes a greater share of the stress in the crack section. High stresses longitudinal to the fibres in the FFRP, close to the strength of the reinforcement are registered around 25 kN.

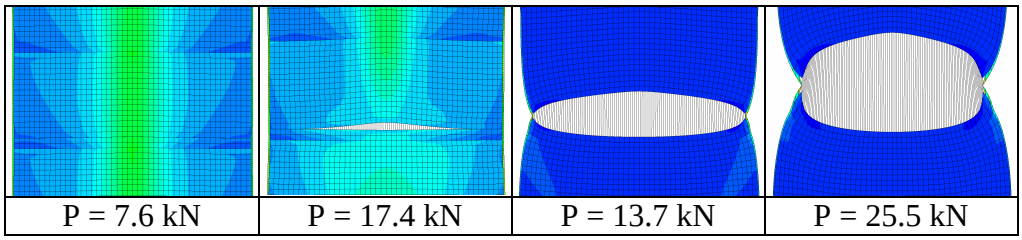

Figure 10: Crack propagation for FFRP reinforced specimens

5. DISCUSSION

The load displacement curves of the linear elastic model, the damage model and the experiment for unreinforced specimen are plotted together in Figure 11. A better estimation of the stiffness in the linear elastic region is given by the model using cohesive elements. The failure in the glulam occurs around 20 kN in the experiments and for the damage model. After failure, the stiffness decrease in both cases.

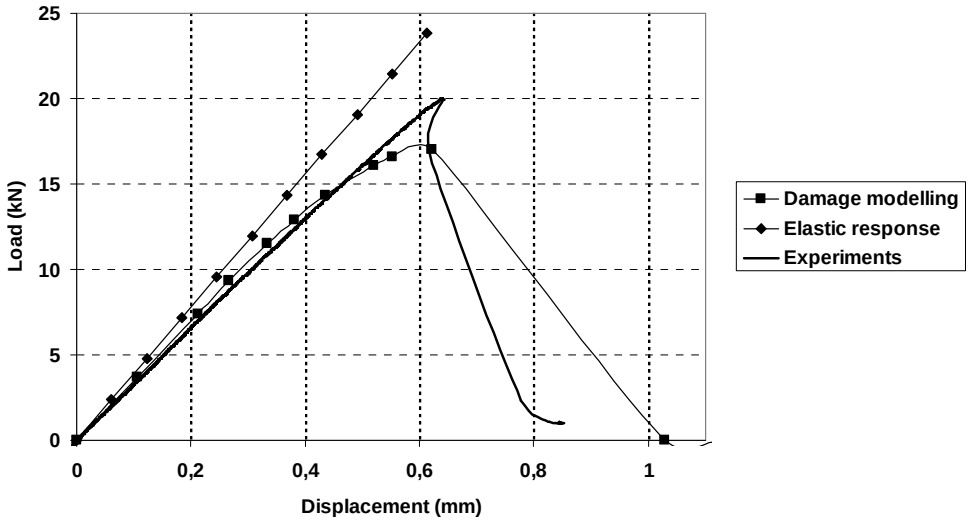

Figure 11: Load displacement curve for damage modelling of unreinforced specimen

The damage modelling with cohesive elements of the FFRP reinforced specimen reveals similarities of the curve pattern with the experimental curve (Figure 12). The load increases until around 20 kN (crack in the glulam), the load decreases after crack initiation followed by a final load increase until fibre failure in the FFRP. However, the displacements are greater in the model, especially the displacement at which the FFRP is activated in the load uptake (1.25 mm in the model against 0.6 during experiments).
The material parameters for the cohesive elements seem to be rather accurate to describe the global behavior of the system under loading perpendicular to the grain. A deeper parametric study would give a better estimation and understanding of these parameters in the system.

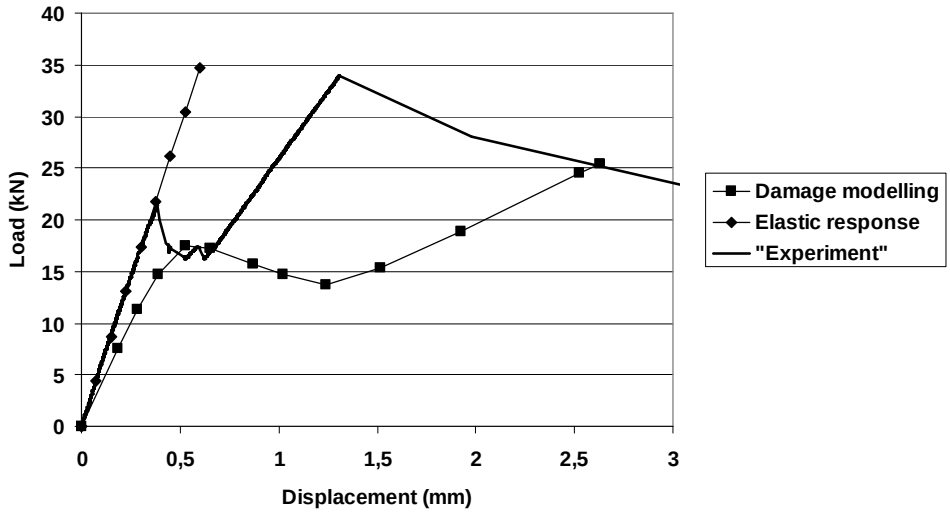

Figure 12: Load displacement curves

6. CONCLUSIONS

The use of flax fibre reinforced polymer as a strengthening device for timber structures has been investigated. Flax Fibre Reinforced Polymer (FFRP) was used as the reinforcement device to strengthen prismatic glulam specimens in tension perpendicular to the grain. The maximum tensile stress perpendicular to the grain was increased by +26 % when the specimens were reinforced with FFRP. The stiffness of the specimens increased for all strengthened specimens. The use of FFRP enhanced the stiffness by +32 %.

For all specimens reinforced with FFRP, higher failure strains were recorded. The specimens had a semi-ductile failure, with warning cracks in the glulam before failure in the fibers.

The tensile stresses perpendicular to grain obtained with Finite Element Analysis can be compared to those from experiments and cohesive elements can be used to model damage initiation and evolution if the section where the crack is most likely to occur is known. A traction separation law was applied successfully.

REFERENCES

1. Gustafsson, P.J., “Timber Engineering”, Chapter 7: Fracture Perpendicular to Grain - Structural Applications, 2003, ISBN 0-470-84469-8.
2. Gutkowski, R. M., Dewey, G. R. and Goodman, J.R., "Full-Scale Test on Double-Tapered Glulam Beams." Journal of the Structural Division, Proceedings of the American Society of Civil Engineers, 1982; 108(10): 2131-2148.
3. Kechter, G.E. and Gutkowski, R.M., "Double-Tapered Glulam Beams: Finite Element Analysis." Journal of Structural Engineering, 1984; 110.
4. Larsen, H. J., Gustafsson, P.J. and Enquist, B., "Tests with glass-fiber reinforcement of wood perpendicular to the grain.", 1992; ISSN 0281-6679.
5. John, K. C. and Lacroix, S., "Composite reinforcement of timber in bending." Can. J. Civ. Eng., 2000; 27: 899-906.
6. Gentile, C., Svecova, D. and Rizkalla, S. H., "Timber beams strengthened with GFRP bars: development and applications." Journal of Composites for Construction, 2002; 6(1): 11-20.
7. Eurocode 5, prEN1995-1-1: Design of timber structures. Part 1-1: General – Common rules and rules for building, Final draft, 2005
8. Larsen, H. J., "“Timber Engineering” –." Chapter12: Design of structure based on Glulam, LVL and other Solid Timber Products, 2003, ISBN 0-470-84469-8.
9. Boström, L., "Method for determination of the softening behaviour of wood and the applicability of a nonlinear fracture mechanics model", 1992, Doctoral Thesis, Report TVBM-1012, Div of Building Materials, Lund University, Sweden.
10. Hillerborg, A., Modeer, M. and Petersson, P.E., "Analysis of crack formation and crack growth in concrete by means of fracture mechanics and finite elements." Cement and Concrete Research, 1976; 6: 773-782.
11. Gustafsson, P.J., "Some tests methods for fracture mechanics properties of wood and qood adhesive joints." Proc. of RILEM TC Workshop on determination of Fracture Mechanics Properties of Wood, 1992
12. Larsen, H. J. and Gustafsson, P.J., "The Fracture Energy of Wood in Tension Perpendicular to the Grain: Results from a Joint Testing Project". International Council for Research and Innovation in Building and Construction, Working Commission CIB-W18, 1990, Lisbon, Portugal.

13. Thelandersson, S., “Timber Engineering” – Chapter 2: Introduction: Wood as a Construction Material, 2003, ISBN 0-470-84469-8.
14. ABAQUS (2006). "V6.6, © ABAQUS, Inc."
15. Blass, H.J. and Schmid, M., "Tensile Strength Perpendicular to Grain of Glued Laminated Timber, 1999" International Council for Research and Innovation in Building and Construction, Working Commission W18-Timber Structures (CIB-W18) – Meeting 32, Graz, Austria.